Quantum chemical investigation of the interaction of the Pt_6 cluster with oxides of different nature

M. N. Mikhailov,[a,b] L. M. Kustov,[a] and V. Z. Mordkovich[b]*

[a]N. D. Zelinsky Institute of Organic Chemistry, Russian Academy of Sciences, 47 Leninsky prosp., 119991 Moscow, Russian Federation. E-mail: mik@ioc.ac.ru
[b]United Research and Development Center, Building 2, 55/1 Leninsky prosp., 119333 Moscow, Russian Federation

The interaction of a Pt_6 nanoparticle with different oxide supports, *viz.*, γ-Al_2O_3, FAU and MFI zeolites, was investigated using the density functional theory. The interaction with the basic oxygen anions of the lattice and with hydroxyl groups of the support affects the electronic structure of the metal particles. The transfer of H atoms of the hydroxyl groups to the metal particle suppresses the Brönsted acidity of the support, and the activation energy of proton transfer decreases with an increase in the acidity of the support. The potential energy profiles were calculated for the transfer processes, and changes in the electronic structures and charge distribution of the supported particles were outlined. The H atom transfer results in positive charging by the metal particles, whereas the interaction with basic sites leads to the appearance of electron-enriched metal clusters.

Key words: platinum particles, alumina, zeolites FAU and MFI, hydrogen spillover, density functional theory.

Fine metal particles on different oxide supports (SiO_2, Al_2O_3, and zeolites) show catalytic activity in (de)hydrogenation,[1,2] isomerization,[3] oxidation,[4—6] and aromatization.[7,8] Metals supported on zeolites are active and stable catalysts of hydrocracking, isomerization, and reforming.[9—14] It is accepted that (de)hydrogenation and ring opening processes occur on a metal particle, whereas isomerization occurs on an acid site.[15,16] However, a strong interaction between the acid site and metal particle has recently[17] been shown. Acid sites of zeolite modify the electronic structure of metal particles, and the presence of platinum results in a decrease in the strength of the acid sites or even in their complete suppression.

To the present time, calculations of the interaction of metal particles with hydroxyl groups of the support were calculated only for the system M_6/H-form of faujasite (M is metal of Group 8—11).[18,19] According to these calculations, metal particles are oxidized by acidic hydroxyl groups of zeolite with the transfer of H atoms of the hydroxyl group to the metal surface. In the later work,[20] the interaction of the Pt atom with the HZSM-5 zeolite was studied at the B3LYP level and the Pt atom was shown to interact with the Brönsted proton and the nearest bridging O atom of the zeolite lattice. Thus, the role played by the support cannot be reduced only to an increase in dispersion of the metal component. However, the nature of interaction between the metal nanoparticles and oxide supports which exhibit different amounts of acid sites with various acid strengths is still far from being undrestood. The Pt_6 particle and oxide supports are convenient objects for studying the interaction of the mutual metal—support influence.

The present work is aimed at studying the metal—support interaction using the density functional theory for the Pt_6 particle and several oxide supports with different properties: γ-Al_2O_3 and zeolites FAU and MFI.

Calculation procedures

The cluster approach was used to describe the structures of the oxides (γ-Al_2O_3, SiO_2, zeolites FAU and MFI). The electronic structures of the clusters were calculated by the density functional theory (DFT) using the exchange B3 functional (see Ref. 21) and correlation LYP [22] and VWN5 [23] (R-B3LYP) functionals. The SBK pseudo-potential[24] and the corresponding basis set augmented by the polarization functions on all atoms were used to decrease the computational time. The calculations were performed using the quantum chemical PC GAMESS program package.[25,26] Natural site populations were analyzed using the NBO program package,[27] and the spectra of state densities were obtained by the AOMix program.[28,29]

Results and Discussion

Pt/γ-Al_2O_3 System. The cluster modeling the surface of partially dehydroxylated alumina is based on the γ-Al_2O_3

Published in Russian in *Izvestiya Akademii Nauk. Seriya Khimicheskaya,* No. 3, pp. 386—394, March, 2007.
1066-5285/07/5603-0397

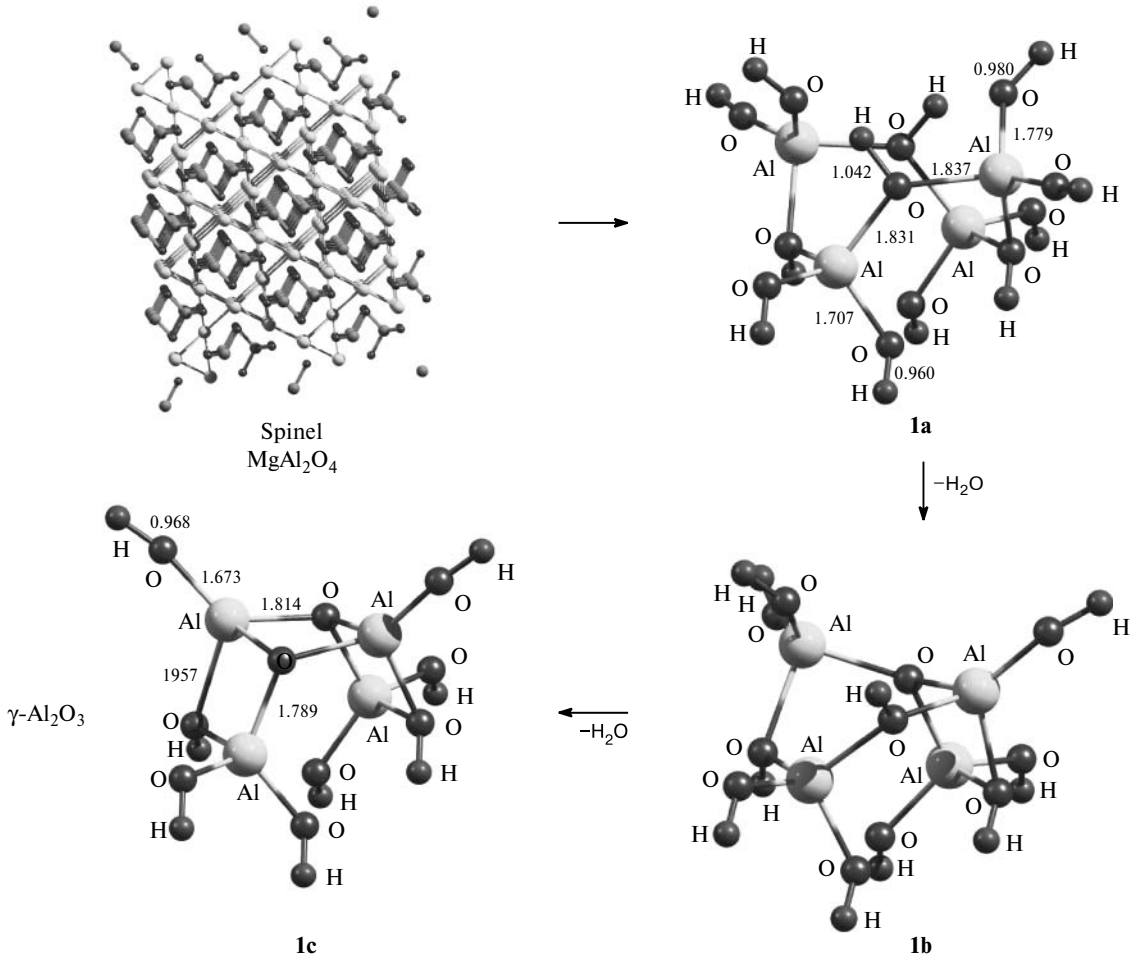

Fig. 1. Cluster (**1c**) modeling the partially dehydroxylated γ-Al_2O_3 surface; interatomic distances (Å) are indicated.

structure.[30,31] The starting structure was that of ideal spinel $MgAl_2O_4$ with the lattice constant corresponding to γ-Al_2O_3 (a = 7.911 Å) in which some Mg atoms were substituted for Al atoms and a leaving part of cationic positions unoccupied. The fragment of the (110) surface containing four Al atoms bound with the O atoms was chosen as a model cluster (Fig. 1).

The broken bonds of the clusters were saturated with H atoms placed at a distance of 0.96 Å from the O atoms along the O—Al bonds of the crystal. During geometry optimization, all terminal OH groups (except for the surface OH groups) were fixed. The optimized structure of the cluster obtained (cluster **1a**) is shown in Fig. 1. The cluster containing two terminal OH groups (cluster **1c**) was chosen for the simulation of the partially dehydroxylated γ-Al_2O_3 surface. Cluster **1c** was obtained by the removal of two water molecules followed by geometry optimization.

The optimized clusters modeling the main intermediates of the interaction process of the platinum particles with the partially hydroxylated alumina surface and the corresponding density of states (DS) spectra of platinum are presented in Fig. 2. The total charges of Pt_6 particles, Fermi energies, and band gaps for structures **2a—c** are given in Table 1.

The natural charges and electronic configurations of atoms in the clusters are given in Table 2. The adsorption interaction of cluster **1c** and the Pt_6 nanoparticle (electronic configuration $5d^{9.41}6s^{0.55}$) is characterized by an energy of 41 kcal mol^{-1} and leads to adsorption complex **2a**. The geometry of both the metal particle and

Table 1. Total charges of Pt_6 particles ($q_n(Pt_6)$), Fermi energies ($E_F = E_{HOMO}$), and band gaps ($E_{bg} = E_{LUMO} - E_{HOMO}$) for compounds **2—4**

Compound	$q_n(Pt_6)$	$-E_F$	E_{bg}	Compound	$q_n(Pt_6)$	$-E_F$	E_{bg}
		eV				eV	
Pt_6	0.0	5.02	1.42	**3b**	0.54	4.60	1.26
2a	0.45	5.26	1.19	**3c**	1.26	5.35	1.22
2b	0.72	5.50	1.17	**3d**	1.89	6.35	1.72
2c	1.05	5.92	1.21	**4a**	−0.21	3.38	1.16
3a	−0.10	4.41	1.23	**4b**	0.51	4.33	1.44

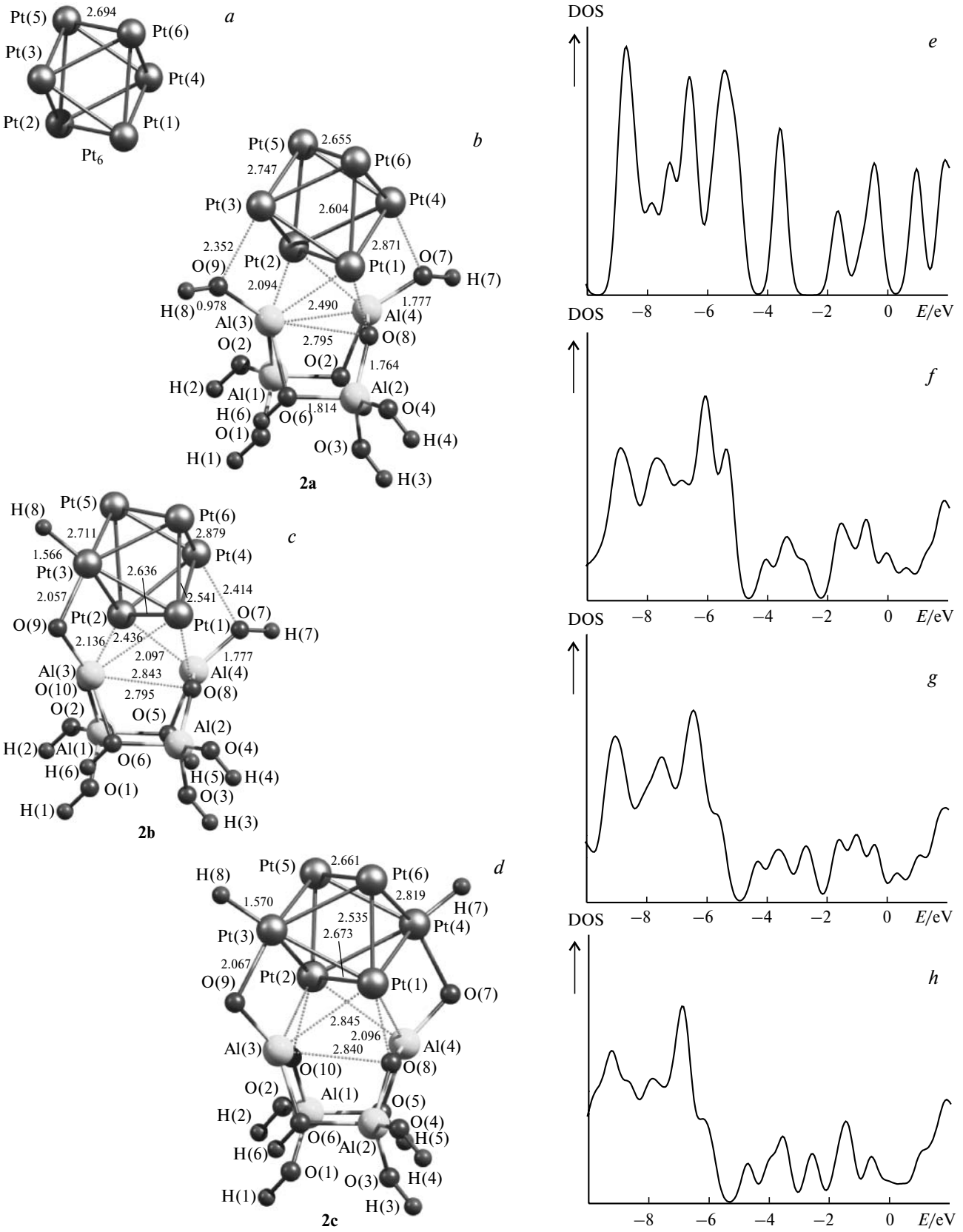

Fig. 2. Optimized structures of intermediates of the interaction of the Pt_6 particles with the γ-Al_2O_3 surface (*a*—*d*) and the corresponding DS spectra of platinum (*e*—*h*).

Table 2. Natural charges (q) and electronic configurations of atoms (in parentheses) in clusters **1c** and **2a—c**

Atom	q			
	1c	**2a**	**2b**	**2c**
O(7)	−1.23 ($2s^{1.73}2p^{5.48}$)	−1.22 ($2s^{1.76}2p^{5.44}$)	−1.21 ($2s^{1.77}2p^{5.43}$)	−1.16 ($2s^{1.86}2p^{5.28}$)
O(8)	−1.43 ($2s^{1.81}2p^{5.61}$)	−1.36 ($2s^{1.79}2p^{5.55}$)	−1.36 ($2s^{1.80}2p^{5.55}$)	−1.36 ($2s^{1.80}2p^{5.55}$)
O(9)	−1.23 ($2s^{1.73}2p^{5.48}$)	−1.22 ($2s^{1.76}2p^{5.44}$)	−1.16 ($2s^{1.86}2p^{5.28}$)	−1.16 ($2s^{1.86}2p^{5.28}$)
O(10)	−1.43 ($2s^{1.81}2p^{5.61}$)	−1.36 ($2s^{1.79}2p^{5.55}$)	−1.37 ($2s^{1.81}2p^{5.55}$)	−1.36 ($2s^{1.80}2p^{5.55}$)
Al(3)	2.16 ($3s^{0.29}3p^{0.53}$)	1.83 ($3s^{0.44}3p^{0.70}$)	1.98 ($3s^{0.38}3p^{0.61}$)	1.97 ($3s^{0.38}3p^{0.62}$)
Al(4)	2.16 ($3s^{0.29}3p^{0.53}$)	1.83 ($3s^{0.44}3p^{0.70}$)	1.86 ($3s^{0.43}3p^{0.68}$)	1.97 ($3s^{0.38}3p^{0.62}$)
H(7)	0.53 ($1s^{0.47}$)	0.53 ($1s^{0.47}$)	0.53 ($1s^{0.47}$)	0.03 ($1s^{0.96}$)
H(8)	0.53 ($1s^{0.47}$)	0.53 ($1s^{0.47}$)	0.04 ($1s^{0.95}$)	0.03 ($1s^{0.96}$)
Pt(1)	—	0.22 ($5d^{9.12}6s^{0.60}$)	0.18 ($5d^{9.03}6s^{0.72}$)	0.23 ($5d^{9.03}6s^{0.67}$)
Pt(2)	—	0.22 ($5d^{9.12}6s^{0.60}$)	0.18 ($5d^{9.10}6s^{0.66}$)	0.23 ($5d^{9.03}6s^{0.67}$)
Pt(3)	—	0.03 ($5d^{9.28}6s^{0.64}$)	0.28 ($5d^{8.90}6s^{0.78}$)	0.27 ($5d^{8.92}6s^{0.76}$)
Pt(4)	—	0.03 ($5d^{9.28}6s^{0.64}$)	0.09 ($5d^{9.24}6s^{0.64}$)	0.27 ($5d^{8.92}6s^{0.76}$)
Pt(5)	—	−0.03 ($5d^{9.31}6s^{0.68}$)	−0.08 ($5d^{9.27}6s^{0.78}$)	0.02 ($5d^{9.20}6s^{0.75}$)
Pt(6)	—	−0.03 ($5d^{9.31}6s^{0.68}$)	0.07 ($5d^{9.21}6s^{0.68}$)	0.02 ($5d^{9.20}6s^{0.75}$)
Pt_6	—	0.45	0.72	1.05

support change substantially due to adsorption: the Pt(1)—Pt(2) bond elongates by 0.2 Å, and the Pt(2)—Pt(3) and Pt(1)—Pt(4) distances increase by 0.15 Å; the Al(3)—O(8) and Al(4)—O(10) bonds elongate by 0.8 Å, and coordination of the Al atom changes from tetrahedral to trigonal. The other geometric parameters change insignificantly.

The Pt_6 particle can be divided into three layers. The Pt(1) and Pt(2) atoms of the first layer interact during adsorption with the basic oxygen anions of the lattice, *viz.*, O(8) and O(10) (Pt—O bond length 2.1 Å), and with the Lewis acid sites Al(3) and Al(4) (Pt—Al bond length 2.5 Å). As a result, the Pt atoms of the first layer are oxidized ($5d^{9.41}6s^{0.55} \rightarrow 5d^{9.12}6s^{0.60}$) acquiring a positive charge of 0.22, and the d-orbitals make the highest contribution to changes in the electron density. As can be seen from the data in Table 1, the electron density on the basic sites (O atoms) decreases ($2s^{1.81}2p^{5.61} \rightarrow 2s^{1.79}2p^{5.55}$) and that on the acid sites (Al atoms) increases ($3s^{0.29}3p^{0.53} \rightarrow 3s^{0.44}3p^{0.70}$). The Pt atoms of the second layer enter into a very weak adsorption interaction with the O atoms of the hydroxyl groups, and the atoms of the third layer, which is most remote from the surface, do not interact with the oxide support. The electron density on the O atoms decreases slightly ($2s^{1.73}2p^{5.48} \rightarrow 2s^{1.76}2p^{5.44}$); nevertheless, the atoms of the second layer are oxidized ($5d^{9.41}6s^{0.55} \rightarrow 5d^{9.28}6s^{0.64}$). The platinum particle is polarized: the atoms of the top layer are negatively charged, and the atoms of the second layer acquire a positive charge. Thus, when interacting with the γ-Al_2O_3 (110) surface, the Pt_6 particle is oxidized to gain a positive charge of 0.45.

It is known[32] that the spillover is observed on the Pt/Al_2O_3 system. This involves adsorption of dihydrogen on metal particle followed by dissociation and migration to the oxide support to form the surface OH groups

$$M_n^{n+} + H_2 \rightarrow M_n^{n+} + 2\,H, \quad (1)$$

$$M_n^{n+} + H + O_s^{2-} \rightarrow M_n^{(n-1)+} + OH_s^-, \quad (2)$$

where M_n is the supported metal particle, OH_s^- is the surface OH group, and O_s^{2-} is the oxygen anion of the oxide cluster. Cluster **2a** contains OH groups formed according to Eq. (2). The interaction of these OH groups with a metal particle can result in the phenomenon named "reverse spillover"

$$M_n^{(n-1)+} + OH_s^- \rightarrow M_n^{n+} + H + O_s^{2-}. \quad (3)$$

The direction of the spillover—reverse spillover process is determined by the nature of the metal.

Let us consider the energy of oxidation of the Pt particle by the H atoms of the surface OH groups. The transfer of the H atom of one of the OH groups to the metal particle surface leads to surface structure **2b**. In cluster **2b**, the Pt(3)—O(9) distance shortens by 0.3 Å and the Pt—O covalent bond is formed. In this case, the adsorbed state of atomic hydrogen ($1s^{0.47} \rightarrow 1s^{0.95}$) with the Pt—H bond length 1.57 Å is formed on the Pt(3) atom. The Pt(3) atom is oxidized ($5d^{9.28}6s^{0.64} \rightarrow 5d^{8.90}6s^{0.78}$) acquiring a charge of 0.28. The charge of the metal particle in the structure with one transferred H atom of the hydroxyl group is 0.72. The transfer of the H atom of the second surface OH group results in the formation of surface platinum cluster **2c** with two adsorbed H atoms ($1s^{0.96}$) on the Pt(3) and Pt(4) atoms; in this structure the metal particle charge increases to 1.05. Hydrogen transfers to the metal particle are endothermic (ΔE_1 = 10 kcal mol^{-1},

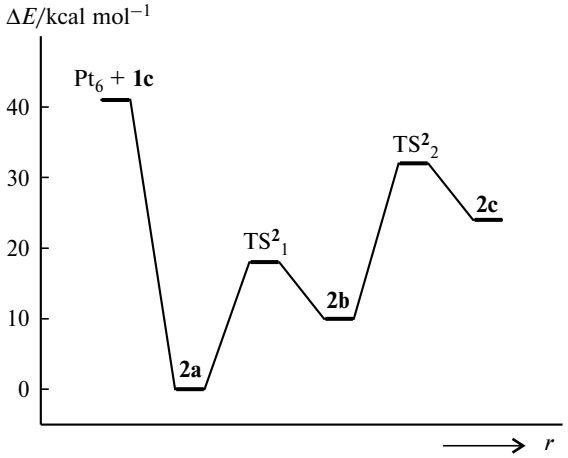

Fig. 3. Cross-section of the potential energy surface for the interaction of the Pt_6 particle with the γ-Al_2O_3 surface; r is the reaction coordinate.

ΔE_2 = 15 kcal mol^{-1}) with activation energies of 18 and 22 kcal mol^{-1}, respectively (Fig. 3).

Thus, in the case of platinum, the hydrogen spillover is thermodynamically more favorable. The interaction of platinum with the alumina surface results in substantial changes in the electronic structure of the metal particle confirmed by analysis of the density of states (see Fig. 2). The data in Fig. 2 show that the interaction of the Pt_6 cluster with the surface OH groups shifts the Fermi level toward higher energies and decreases the band gap. Hydrogen transfer followed by Pt—O bond formation induces the shift of the d-band of platinum toward higher binding energies accompanied by an increase in the ionization energy, whereby the band gap remains virtually unchanged.

Pt/FAU System. The cluster modeling the fragment of the FAU zeolite framework is based on the six-membered ring, *viz.*, fragment of a large cavity. The cluster model contains three Si atoms and three Al atoms arranged alternately according to the Löwenstein rule.[33] The coordinates of nuclei are chosen according to the known crystallographic data.[34] The broken Si—O and Al—O bonds of the cluster are saturated with the H atoms placed at distances of 0.96 Å along the Al—O and Si—O bonds, respectively. All terminal OH groups were fixed during geometry optimization. An excessive positive charge of the lattice is compensated by three protons that form three bridging acidic OH groups of the zeolite. The resulting cluster has stoichiometry $Al_3Si_3O_{18}H_{15}$.

The optimized clusters modeling the main intermediates of interaction process of the platinum particle with the fragment of the FAU zeolite and the corresponding spectra of the density of states of platinum are presented in Fig. 4. The total charges of the particles, Fermi energies, and band gaps for structures **3a—d** are given in Table 1. The natural charges and electronic configurations of atoms in the clusters are given in Table 3. The adsorption interaction of the zeolite cluster and Pt_6 nanoparticle (electronic configuration $5d^{9.41}6s^{0.55}$) affording adsorption complex **3a** is characterized by an adsorption energy of 22 kcal mol^{-1}, which is half of that of alumina. The geometry of the metal particle change considerably due to adsorption: the Pt(2)—Pt(3) bond elongates by 0.2 Å, and the Pt(1)—Pt(6) and Pt(2)—Pt(5) distances increase by 0.08 and 0.13 Å, respectively; the Al—O and Si—O bonds somewhat shorten (by 0.02—0.04 Å), and the O—H bonds of the bridging groups elongate by 0.1 Å. The other geometric parameters change insignificantly. During adsorption the Pt(1), Pt(2), and Pt(3) atoms of the Pt_6 particle interact with the oxygen atoms of the lattice, *viz.*, O(13), O(15), and O(17) (Pt—O bond length 2.3—2.5 Å). and with protons of the Brönsted acid sites H(13), H(14), and H(15) (the Pt(2)—H(13) bond length is 2.27 Å, and the Pt(3)—H(14) and Pt(1)—H(15) bonds are longer by 0.25 Å). As a result, the Pt particle acquires a small negative charge. As can be seen from the data in Table 2, the electron density on the Si atoms slightly decreases and that on the Brönsted acid sites increases. The metal cluster is additionally stabilized due to the donation of an excessive electron density to the acid sites.

The transfer of one of the Brönsted protons (H(13)) to the metal particle surface results in surface structure **3b**. In cluster **3b** the Pt(1)—O(13) distance shortens by 0.25 Å, and the adsorbed state of hydrogen atoms ($1s^{0.47} \rightarrow 1s^{1.01}$) with the Pt(2)—H(13) and Pt(6)—H(13) bond lengths equal to 1.68 and 1.75 Å, respectively, is formed at the Pt(2)—Pt(6) edge. The Pt(1) ($5d^{9.31}6s^{0.62} \rightarrow 5d^{9.07}6s^{0.57}$) and Pt(2) ($5d^{9.29}6s^{0.67} \rightarrow 5d^{9.09}6s^{0.55}$) atoms are oxidized to acquire charges of 0.31 and 0.30, respectively, whereas the electronic state of the Pt(6) atoms remains almost unchanged. The charge of the Pt_6 particle increases to 0.54. The transfer of protons of other acid sites affords complexes **3c** and **3d** with two and three adsorbed H atoms, respectively (see Fig. 4 and Table 2). In this case, the Pt—O bonds between the Pt atoms of the layer nearest to the layer surface (Pt(1), Pt(2), and Pt(3)) and oxygen atoms of the lattice (O(13), O(15), and O(17)) shorten. As a result of transfer of the Brönsted protons, the atoms of the first layer are oxidized (charges 0.48, 0.58, and 0.59), whereas the atoms of the top layer bear but a small positive charge. The total charge of the Pt particle in complexes **3c** and **3d** increases to 1.26 and 1.89, respectively. The Brönsted proton transfers to the platinum cluster are exothermic, and the transfer energy decreases accordingly: 23, 12, and 9 kcal mol^{-1}. The activation energies of the proton transfer are 9—14 kcal mol^{-1} (Fig. 5). Thus, for the interaction of the platinum cluster with the FAU zeolite fragment the reverse hydrogen spillover is thermodynamically favorable. The evidence of the metal—support interaction is observed: the metal particle is oxidized

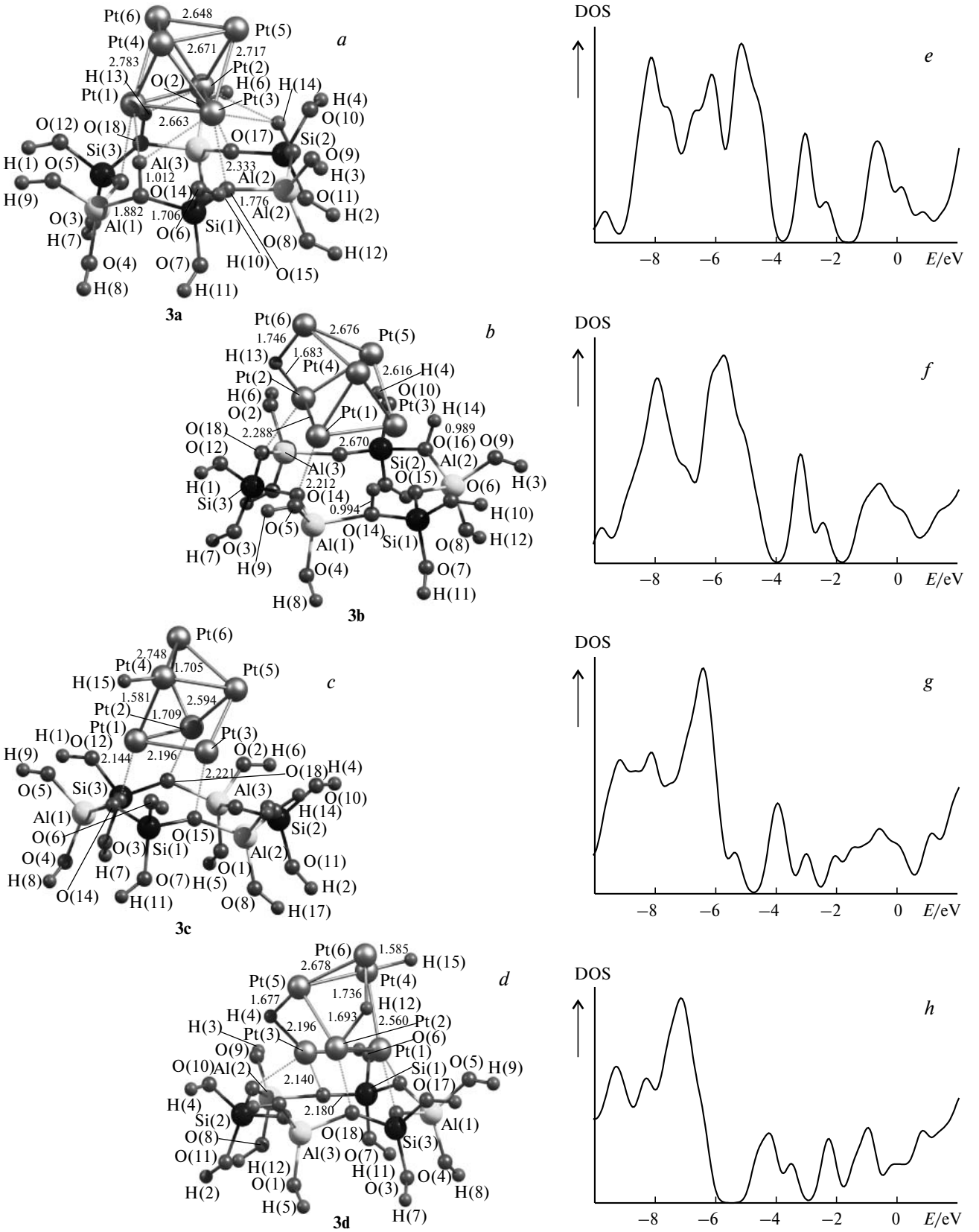

Fig. 4. Optimized structures of intermediates of the interaction of the Pt_6 particle with the FAU zeolite **3a—d** (*a—d*) and the corresponding DS spectra of platinum (*e—h*).

Table 3. Natural charges (q) and electronic configurations of atoms (in parentheses) in the FAU clusters and clusters **3a—d**

Atom	q				
	FAU	**3a**	**3b**	**3c**	**3d**
O(13)	−1.33 ($2s^{1.78}2p^{5.54}$)	−1.34 ($2s^{1.78}2p^{5.55}$)	−1.31 ($2s^{1.78}2p^{5.53}$)	−1.28 ($2s^{1.78}2p^{5.49}$)	−1.27 ($2s^{1.78}2p^{5.47}$)
O(14)	−1.15 ($2s^{1.74}2p^{5.40}$)	−1.17 ($2s^{1.75}2p^{5.41}$)	−1.16 ($2s^{1.74}2p^{5.40}$)	−1.34 ($2s^{1.77}2p^{5.56}$)	−1.31 ($2s^{1.78}2p^{5.51}$)
O(15)	−1.33 ($2s^{1.78}2p^{5.54}$)	−1.33 ($2s^{1.78}2p^{5.54}$)	−1.32 ($2s^{1.78}2p^{5.53}$)	−1.33 ($2s^{1.78}2p^{5.53}$)	−1.26 ($2s^{1.78}2p^{5.48}$)
O(16)	−1.15 ($2s^{1.74}2p^{5.40}$)	−1.18 ($2s^{1.75}2p^{5.42}$)	−1.16 ($2s^{1.74}2p^{5.40}$)	−1.16 ($2s^{1.75}2p^{5.39}$)	−1.23 ($2s^{1.78}2p^{5.43}$)
O(17)	−1.33 ($2s^{1.78}2p^{5.54}$)	−1.33 ($2s^{1.78}2p^{5.54}$)	−1.33 ($2s^{1.78}2p^{5.54}$)	−1.33 ($2s^{1.78}2p^{5.54}$)	−1.36 ($2s^{1.78}2p^{5.57}$)
O(18)	−1.15 ($2s^{1.74}2p^{5.40}$)	−1.18 ($2s^{1.75}2p^{5.42}$)	−1.32 ($2s^{1.77}2p^{5.53}$)	−1.30 ($2s^{1.78}2p^{5.51}$)	−1.29 ($2s^{1.78}2p^{5.50}$)
Al(1)	2.10 ($3s^{0.30}3p^{0.57}$)	2.10 ($3s^{0.29}3p^{0.58}$)	2.10 ($3s^{0.29}3p^{0.59}$)	2.07 ($3s^{0.29}3p^{0.61}$)	2.07 ($3s^{0.29}3p^{0.60}$)
Al(2)	2.10 ($3s^{0.30}3p^{0.57}$)	2.10 ($3s^{0.29}3p^{0.58}$)	2.11 ($3s^{0.29}3p^{0.57}$)	2.11 ($3s^{0.29}3p^{0.57}$)	2.07 ($3s^{0.29}3p^{0.61}$)
Al(3)	2.10 ($3s^{0.30}3p^{0.57}$)	2.10 ($3s^{0.29}3p^{0.58}$)	2.07 ($3s^{0.29}3p^{0.61}$)	2.08 ($3s^{0.29}3p^{0.60}$)	2.08 ($3s^{0.29}3p^{0.60}$)
Si(1)	2.53 ($3s^{0.46}3p^{0.94}$)	2.55 ($3s^{0.46}3p^{0.92}$)	2.55 ($3s^{0.46}3p^{0.92}$)	2.55 ($3s^{0.46}3p^{0.92}$)	2.57 ($3s^{0.46}3p^{0.90}$)
Si(2)	2.53 ($3s^{0.46}3p^{0.94}$)	2.55 ($3s^{0.46}3p^{0.92}$)	2.55 ($3s^{0.46}3p^{0.93}$)	2.55 ($3s^{0.46}3p^{0.93}$)	2.55 ($3s^{0.46}3p^{0.93}$)
Si(3)	2.53 ($3s^{0.46}3p^{0.94}$)	2.55 ($3s^{0.46}3p^{0.92}$)	2.55 ($3s^{0.45}3p^{0.93}$)	2.55 ($3s^{0.46}3p^{0.92}$)	2.56 ($3s^{0.46}3p^{0.92}$)
H(13)	0.55 ($1s^{0.45}$)	0.53 ($1s^{0.47}$)	−0.02 ($1s^{1.01}$)	0.00 ($1s^{1.00}$)	0.00 ($1s^{0.99}$)
H(14)	0.55 ($1s^{0.45}$)	0.54 ($1s^{0.45}$)	0.55 ($1s^{0.45}$)	0.55 ($1s^{0.45}$)	−0.08 ($1s^{1.07}$)
H(15)	0.55 ($1s^{0.45}$)	0.54 ($1s^{0.45}$)	0.55 ($1s^{0.44}$)	−0.02 ($1s^{1.02}$)	−0.05 ($1s^{1.04}$)
Pt(1)	—	0.00 ($5d^{9.31}6s^{0.62}$)	0.31 ($5d^{9.07}6s^{0.57}$)	0.54 ($5d^{8.89}6s^{0.51}$)	0.59 ($5d^{8.76}6s^{0.59}$)
Pt(2)	—	−0.02 ($5d^{9.29}6s^{0.67}$)	0.30 ($5d^{9.09}6s^{0.55}$)	0.39 ($5d^{8.96}6s^{0.59}$)	0.48 ($5d^{8.91}6s^{0.56}$)
Pt(3)	—	−0.06 ($5d^{9.31}6s^{0.69}$)	−0.08 ($5d^{9.24}6s^{0.79}$)	0.31 ($5d^{9.04}6s^{0.59}$)	0.58 ($5d^{8.83}6s^{0.54}$)
Pt(4)	—	−0.02 ($5d^{9.37}6s^{0.61}$)	0.03 ($5d^{9.23}6s^{0.70}$)	−0.02 ($5d^{9.10}6s^{0.88}$)	0.15 ($5d^{8.98}6s^{0.84}$)
Pt(5)	—	−0.01 ($5d^{9.44}6s^{0.54}$)	0.00 ($5d^{9.34}6s^{0.62}$)	−0.02 ($5d^{9.19}6s^{0.78}$)	0.00 ($5d^{9.19}6s^{0.76}$)
Pt(6)	—	0.01 ($5d^{9.32}6s^{0.63}$)	−0.02 ($5d^{9.42}6s^{0.58}$)	0.06 ($5d^{9.42}6s^{0.51}$)	0.09 ($5d^{9.28}6s^{0.62}$)
Pt_6	—	−0.10	0.54	1.26	1.89

and the number and strength of the Brönsted acid sites in the zeolite decrease. Analysis of the density of states spectra for metal particle (see Fig. 4, Table 1) shows that the immobilization of the Pt_6 cluster in the FAU zeolite cavity induces the shift of the Fermi level toward lower energies by 0.6 eV and a decrease in the band gap. The transfer of the Brönsted protons to the metal particle shifts the Fermi level toward higher energies to −6.35 eV and increases the band gap to 1.72 eV.

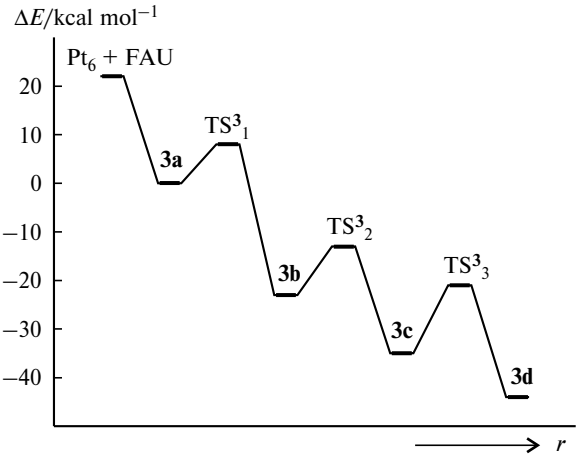

Fig. 5. Cross-section of the potential energy surface for the interaction of the Pt_6 particle with the FAU zeolite fragment; r is the reaction coordinate.

Pt/MFI System. The cluster modeling the fragment of the MFI zeolite framework is based on the ten-membered ring from the straight zeolite channel at the intersection with the sinusoidal channel. The cluster model includes fourteen Si atoms and one Al atom. The broken bonds (Si—O and Al—O) of the cluster are saturated with the H atoms placed at distances of 1.6 and 1.5 Å along the Al—O and Si—O, respectively. All terminal H atoms are fixed during geometry optimization. The excessive positive charge of the lattice was compensated by the proton forming the bridging acidic O(18)H(25) group of the zeolite. The cluster obtained has stoichiometry $AlSi_{14}O_{18}H_{25}$.

The optimized clusters modeling the main intermediates of the interaction process of the platinum particle with the ZSM-5 (MFI) zeolite fragment and the corresponding DS of the state densities of platinum are presented in Fig. 6. The total charges of Pt_6 particles, Fermi energies, and band gaps for structures **4a,b** are given in Table 1. The natural charges and electronic configurations of atoms in the clusters are presented in Table 4. The adsorption of the MFI zeolite and Pt_6 nanoparticle (electronic configuration $5d^{9.41}6s^{0.55}$) is characterized by a very low adsorption energy (6 kcal mol^{-1}) and affords adsorption complex **4a**. As a result, the geometry of the metal particle change significantly: the Pt(1)—Pt(5), Pt(1)—Pt(6), Pt(2)—Pt(4), and Pt(2)—Pt(3) bonds shorten by 0.12—0.18 Å, and the Pt(1)—Pt(4), Pt(2)—Pt(5), Pt(2)—Pt(6), Pt(1)—Pt(3), and

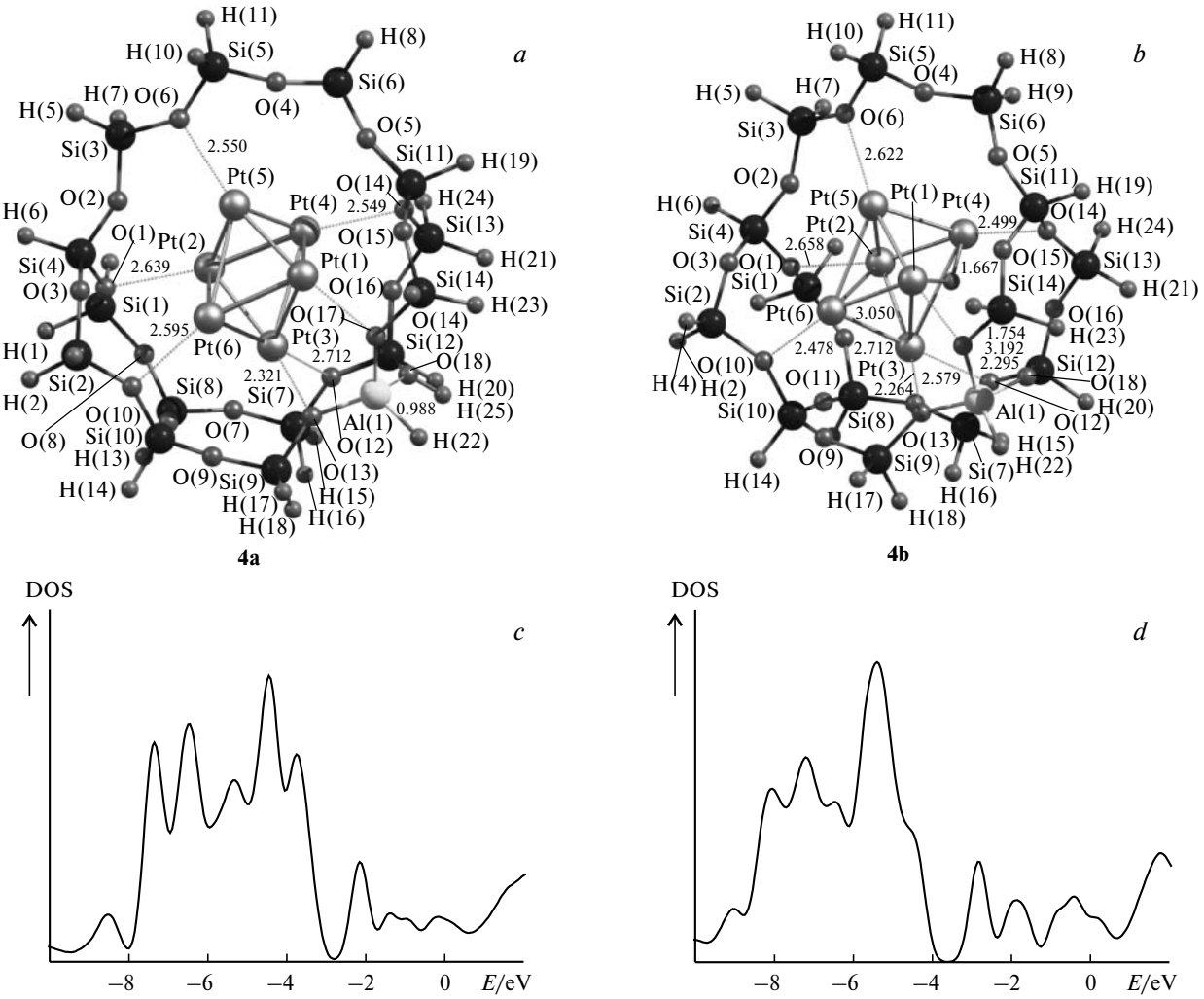

Fig. 6. Optimized structures of intermediates of the interaction of the Pt_6 particle with the MFI zeolite **4a,b** (*a*, *b*) and the corresponding DS spectra of platinum (*c*, *d*).

Table 4. Natural charges and electronic configurations of atoms (in parentheses) in the MFI clusters and clusters **4a,b**

Atom	*q*			Atom	*q*		
	MFI	**4a**	**4b**		MFI	**4a**	**4b**
O(12)	−1.29 ($2s^{1.74}2p^{5.55}$)	−1.30 ($2s^{1.73}2p^{5.55}$)	−1.31 ($2s^{1.75}2p^{5.55}$)	Pt(1)	—	0.04 ($5d^{9.28}6s^{0.63}$)	0.21 ($5d^{9.12}6s^{0.62}$)
O(13)	−1.35 ($2s^{1.76}2p^{5.58}$)	−1.37 ($2s^{1.76}2p^{5.60}$)	−1.36 ($2s^{1.76}2p^{5.58}$)	Pt(2)	—	−0.10 ($5d^{9.42}6s^{0.63}$)	−0.08 ($5d^{9.35}6s^{0.69}$)
O(17)	−1.35 ($2s^{1.76}2p^{5.58}$)	−1.36 ($2s^{1.76}2p^{5.59}$)	−1.34 ($2s^{1.77}2p^{5.55}$)	Pt(3)	—	−0.05 ($5d^{9.34}6s^{0.65}$)	0.22 ($5d^{9.16}6s^{0.56}$)
O(18)	−1.15 ($2s^{1.74}2p^{5.39}$)	−1.16 ($2s^{1.74}2p^{5.40}$)	−1.37 ($2s^{1.76}2p^{5.60}$)	Pt(4)	—	−0.15 ($5d^{9.46}6s^{0.63}$)	0.03 ($5d^{9.32}6s^{0.60}$)
Al(1)	1.87 ($3s^{0.45}3p^{0.66}$)	1.90 ($3s^{0.43}3p^{0.64}$)	1.90 ($3s^{0.44}3p^{0.63}$)	Pt(5)	—	0.03 ($5d^{9.34}6s^{0.58}$)	0.10 ($5d^{9.30}6s^{0.56}$)
Si(12)	2.24 ($3s^{0.62}3p^{1.08}$)	2.26 ($3s^{0.61}3p^{1.07}$)	2.24 ($3s^{0.62}3p^{1.08}$)	Pt(6)	—	0.02 ($5d^{9.38}6s^{0.55}$)	0.05 ($5d^{9.28}6s^{0.62}$)
H(25)	0.54 ($1s^{0.46}$)	0.54 ($1s^{0.46}$)	0.01 ($1s^{0.99}$)	Pt_6	—	−0.21	0.51

Pt(3)—Pt(4) bonds elongate by 0.12—0.26 Å. The Al—O and Si—O bond lengths of the zeolite framework change by 0.01—0.02 Å. The cluster particle is localized in the MFI zeolite channel and interacts with the O atoms of the lattice (Pt—O bond lengths 2.3—2.6 Å). Accordingly, the electronic density on the s- and d-orbitals of the Pt(2), Pt(3), and Pt(4) atoms increases (see Table 4). The Pt(1), Pt(5), and Pt(6) atoms bear small positive charges.

As a whole, the Pt_6 cluster is polarized and has a negative total charge. This charge appears due to the electron density redistribution from the Si and Al atoms through the O atoms of the zeolite framework to the metal particle. The transfer of the Brönsted proton (H(25)) to the metal particle surface yields surface structure **4b**. In cluster **4b** the Pt(2)—Pt(6), Pt(1)—Pt(4), and Pt(1)—Pt(3) bonds elongate by 3.02—3.10 Å, and the Pt(3)—Pt(4) distance increases by 3.19. The adsorbed state of atomic hydrogen ($1s^{0.46} \rightarrow 1s^{0.99}$) with the Pt(1)—H(25) and Pt(4)—H(25) bond lengths equal to 1.75 and 1.67 Å, respectively, is formed at the Pt(1)—Pt(4) edge. The Pt(1) ($5d^{9.28}6s^{0.63} \rightarrow 5d^{9.12}6s^{0.62}$) and Pt(4) ($5d^{9.34}6s^{0.65} \rightarrow$ $\rightarrow 5d^{9.16}6s^{0.56}$) atoms are oxidized acquiring charges of 0.21 and 0.22, respectively. The decrease in the electron density is also observed on other Pt atoms. The charge of the metal particle with the transferred Brönsted proton is 0.51. The processes of Brönsted proton transfer to the platinum cluster are exothermic and activation-free, and the transfer energy is equal to 47 kcal mol^{-1}, which exceeds the energy of transfer of three protons in faujasite (44 kcal mol^{-1}). Analysis of the DS spectra of the metal particle (see Fig. 6) shows that the immobilization of the Pt_6 cluster in the MFI zeolite channel induces the shift of the Fermi level toward lower energies by 1.64 eV and an increase in the band gap by 0.26 eV. The transfer of the Brönsted proton to the metal particle results in the shift of the Fermi level toward higher binding energies to –4.33 eV and increases the band gap to 1.44 eV. As a result, the Pt_6 cluster with the transferred proton is characterized by the Fermi level that is 0.69 eV higher than that of the isolated Pt_6 particle and the band gap coincides with that for the isolated cluster.

Thus, the introduction of platinum into the ZSM-5 type zeolite results in a substantial decrease in the number of Brönsted acid sites or even in their complete suppression. Moreover, the interaction of platinum with extra-framework aluminum is accompanied by a decrease in the Lewis acidity of the zeolite. Therefore, it can be assumed that the active sites of the Pt/ZSM-5 catalyst are the adduct of the oxidized metal cluster and H atom.

* * *

The interaction with the basic oxygen anions of the lattice and with the OH groups of the support affects the electronic structure of the metal particles. The transfer of the H atoms of the hydroxyl groups to the metal particle induces the suppression of the Brönsted acidity of the support, and the activation energy of proton transfer decreases with an increase in the acidity of the support. Due to the H atom transfer the metal particle acquires a positive charge, whereas the interaction with the basic sites results in the appearance of electron-enriched metal clusters.

The authors are grateful to Prof. G. M. Zhidomirov for interest in the work and helpful discussion of the results.

References

1. J. Bandiera, C. Naccache, and B. Imelik, *J. Chim. Phys.—Chim. Biol.*, 1978, **75**, 406.
2. J. Chupin, N. S. Gnep, S. Lacombe, and M. Guisnet, *Appl. Catal., A*, 2001, **206**, 43.
3. E. Blomsma, J. A. Martens, and P. A. Jacobs, *Stud. Surf. Sci. Catal. B*, 1997, **105**, 909.
4. M. Watanabe, H. Uchida, H. Igarashi, and M. Suzuki, *Chem. Lett.*, 1995, 21.
5. M. Iwamoto, A. M. Hernandez, and T. Zengyro, *Chem. Commun. (Cambridge)*, 1997, 37.
6. E. V. Benvenutti, L. Franken, C. C. Moro, and C. U. Davanzo, *Langmuir*, 1999, **15**, 37.
7. R. J. Davis, *Heterog. Chem. Rev.*, 1994, **1**, 41.
8. J.-L. Dong, J.-H. Zhu, and Q.-H. Xu, *Appl. Catal., A*, 1994, **112**, 105.
9. L. B. Galperin, J. C. Bricker, and J. R. Holmgren, *Appl. Catal., A*, 2003, **239**, 297.
10. M. Sugioka, C. Tochiyama, Y. Matsumoto, and F. Sado, *Stud. Surf. Sci. Catal.*, 1995, **94**, 544.
11. T. V. Vasina, O. V. Masloboishchikova, E. G. Khelkovskaya-Sergeeva, L. M. Kustov, and J. I. Houzvička, *Stud. Surf. Sci. Catal.*, 2001, **135**, 4207.
12. M. A. Arribas and A. Martinez, *Appl. Catal., A*, 2002, **230**, 203.
13. N. J. Noordhoek, D. Schuring, F. J. M. M. de Gauw, B. G. Anderson, A. M. de Jong, M. J. A. de Voigt, and R. A. van Santen, *Ind. Eng. Chem. Res.*, 2002, **41**, 1973.
14. P. N. Kuznetsov, *J. Catal.*, 2003, **218**, 2.
15. P. B. Weisz and E. W. Swegler, *Science*, 1957, **126**, 31.
16. A. Kuhlmann, F. Roessner, W. Schwieger, O. Gravenhorst, and T. Selvam, *Catal. Today*, 2004, **97**, 303.
17. D. Kubička, N. Kumar, T. Venäläinen, H. Karhu, I. Kubičková, H. Österholm, and D. Yu. Murzin, *J. Phys. Chem., B*, 2006, **110**, 4937.
18. G. N. Vayssilov, B. C. Gates, and N. Rösch, *Angew. Chem., Int. Ed.*, 2003, **42**, 1391.
19. G. N. Vayssilov and N. Rösch, *Phys. Chem. Chem. Phys.*, 2005, **7**, 4019.
20. P. Treesukol, K. Srisuk, J. Limtrakul, and T. N. Truong, *J. Phys. Chem., B*, 2005, **109**, 11940.
21. A. D. Becke, *J. Chem. Phys.*, 1993, **98**, 5648.
22. C. Lee, W. Yang, and R. G. Parr, *Phys. Rev. B*, 1988, **37**, 785.
23. S. H. Vosko, L. Wilk, and M. Nusair, *Can. J. Phys.*, 1980, **58**, 1200.

24. W. J. Stevens, M. Krauss, H. Basch, and P. G. Jasien, *Can. J. Chem.*, 1992, **70**, 612.
25. M. W. Schmidt, K. K. Baldridge, J. A. Boatz, S. T. Elbert, M. S. Gordon, J. J. Jensen, S. Koseki, N. Matsunaga, K. A. Nguyen, S. Su, T. L. Windus, M. Dupuis, and J. A. Montgomery, *J. Comput. Chem.*, 1993, **14,** 1347.
26. A. A. Granovsky, *PC GAMESS Version 7.0*, http://classic.chem.msu.su/gran/gamess/index.html
27. E. D. Glendening, J. K. Badenhoop, A. E. Reed, J. E. Carpenter, and F. Weinhold, *NBO 4. M*, Theoretical Chemistry Institute, University of Wisconsin, Madison (WI), 1999.
28. S. I. Gorelsky, *AOMix: Program for Molecular Orbital Analysis*, http://www.sg-chem.net/, York University, Toronto (Canada), 1997.
29. S. I. Gorelsky and A. B. P. Lever, *J. Organomet. Chem.*, 2001, **187**, 635.
30. O. Maresca, A. Allouche, J. P. Aycard, M. Rajzmann, S. Clemendot, and F. Hutschka, *J. Mol. Struct. (THEOCHEM)*, 2000, **505**, 81.
31. E. J. W. Verwey, *Z. Kristallogr.*, 1935, **91**, 317.
32. W. C. Conner, Jr., and J. L. Falconer, *Chem. Rev.*, 1995, **95**, 759.
33. W. Löwenstein, *Am. Mineral.*, 1954, **39**, 92.
34. D. H. Olson, *Zeolites*, 1995, **15**, 439.

Received February 19, 2007;
in revised form February 26, 2007